

Regular article

Modeling the cluster formation during infrared and ultraviolet matrix-assisted laser desorption ionization of oligonucleotides in succinic acid matrix with molecular mechanics

Sandor Kristyan¹, Akos Bencsura¹, Akos Vertes²

¹Chemical Research Center, Institute of Chemistry, Hungarian Academy of Sciences, 1025 Budapest, Pusztaszeri út 59–67, Hungary

²Department of Chemistry, George Washington University, 725. 21st Street, NW, Washington, DC 20052, USA

Revised: 12 October 2001 / Accepted: 27 February 2002 / Published online: 13 June 2002

© Springer-Verlag 2002

Abstract. A large succinic acid ($\text{HOOC}(\text{CH}_2)_2\text{COOH}$) matrix containing $7 \times 7 \times 7$ unit cells with guest oligonucleotide AGCAGCT was modeled with molecular dynamics simulation for infrared matrix-assisted laser desorption ionization. We simulated the laser heating of the succinic acid (this data is still missing from the literature) with $\lambda = 2.94 \mu\text{m}$ infrared laser pulses and compared it to ultraviolet excitation. We did this in order to elucidate the cluster formation of succinic acid in the gas phase in itself and around the analyte. At this wavelength, the laser energy is coupled into the matrix through the OH vibrations of the carboxyl groups. The most pronounced difference we observed at 1,500 K simulation is that infrared heating generates about 10–15 more succinic acid molecules bound to the analyte in noncovalent complex form than the ultraviolet mode, which generates about 2 molecules thus bound. We report energy redistribution within the matrix between the host and guest species as well as other dynamical properties. The parameter and topology data for succinic acid that we used are reported and ready for use in CHARMM computer code environment for simulation.

Key words: Modeling matrix-assisted laser desorption ionization – Molecular mechanics – Clusters – Succinic acid

Introduction

Matrix-assisted laser desorption ionization (MALDI) combined with mass spectrometry is a powerful tool in the characterization of bio- and synthetic polymers. In this technique the volatilization can be achieved up to 200 kDa. The large guest molecule (analyte) is embedded into crystals of relatively small organic molecules

that readily absorb the incident infrared (IR) or ultraviolet (UV) laser light. The process is a collective effect, rather than a sequence of collisions between particles, and as a consequence, many more particles (several hundred at least) are needed in the simulation. Despite the recent dramatic development in the field with respect to available mass range and possible resolution, the theory in this field is somewhat behind. Due to the large number of particles, simulation with molecular mechanics is the only available tool for modeling, as opposed to the more accurate but unfeasible *ab initio* calculations. The simulation not only allows energy, temperature and velocity distributions as well as other quantities to be calculated, but it can also provide a picture of the molecular motions involved in the MALDI processes. Simulation of molecular solids is frequently required as a part of the calculation.

Due to computational limitations in the molecular dynamics (MD) of large molecules, a trade off needs to be found between the size of the system and inclusion of the internal structure. In our original approach to modeling the MALDI process, we selected a widely used MD code (CHARMM) [1] that enabled us to incorporate the internal structure of molecules in MALDI [2]. In this way, IR excitation through vibrational modes as well as UV excitation can be theoretically investigated. The major simplifications such as no fragmentation, ionization and/or electronic excitation, necessarily come from the known drawback of any molecular mechanics method. These drawbacks, which limit the result, do not allow a fair comparison with mass spectrometric data. However MD is still the most up to date method for considering systems with a large number of particles. On the other hand, its advantage is that energy transfer, complexation, IR and UV excitation can be modeled. If the internal structure is not included (e.g. breathing sphere model [3]) the system can be even larger, but features like IR excitation, or certain aspects of cluster formation cannot be considered in detail.

The CHARMM code, originally developed for protein folding and active site dynamics in aqueous envi-

Correspondence to: S. Kristyan, A. Vertes
e-mail: kristyans@chemres.hu, vertes@gwu.edu

ronment, is written for general purposes. For example it can be used to investigate macromolecules embedded in the environment of small molecules. To reduce the number of required interactions the CHARMM program uses the “extended atom representation” which treats certain hydrogen atoms together with neighboring heavy atoms as one “extended particle”. This simplification reduces the large number of pair potentials, while the backbone and function groups of the molecules (in this work, the analyte and matrix molecules) are still in chemical effect.

Succinic acid is known as one of the most utilized general-purpose matrices for IR-MALDI. Experimental data is available for its crystal structure but the modeling of its structure and laser-heating dynamics have not yet been addressed in the literature. The objective of our work was to model the succinic acid MALDI matrix with the analyte embedded in it, and to explore some of its properties with respect to cluster formation. Using the available crystallographic data for succinic acid [4], we modeled the matrix and guest molecules with their detailed molecular structure. The choice of guest molecule originated in our earlier and ongoing research, where certain oligonucleotides are examined because of their affinity for forming noncovalent complexes with peptides via their thymidine content, affected by the acidity of the matrix [5]. In the chosen AGCAGCT oligonucleotide the phosphate link between C and T contained a negative charge, while all succinic acids in the crystal generation and molecular dynamics simulation were neutral molecules. The reason for the choice of this phosphate ionization state has also been addressed in [5].

Methods and calculation

The c24b2 version of CHARMM was used in the calculation [1]. As mentioned, polar hydrogen atoms were represented explicitly whereas non-polar groups were modeled as extended atoms. Bond stretching and bending, dihedral, improper, electrostatic, and van der Waals energy terms were considered in the empirical potential energy function. The succinic acid and oligonucleotide (AGCAGCT) were represented by their detailed molecular structure. Before any energy calculation, we redefined the non-bond cutoff values and cutoff methods against the default properties. Instead of rewriting the suggested parameter files from the CHARMM library, we used the command “ENERGY CDIE INBFRQ -1 cutnb 14.0 ctofnb 12.0 ctonnb 8.0 fswitch vswitch cutim 16.0”. Our experience is that this works the best for energy calculations, at least in the case of MALDI-related calculations and materials.

Since succinic acid was not in the CHARMM parameter set, we used *ab initio* quantum chemical calculations [6] (GAMESS at 3-21G* basis level) to determine its structural parameters and ChelpG partial charge [7, 10, 11, 12, 13] distribution. One of the key results of this paper is the calculation of optimized data for succinic acid as molecule or solid for CHARMM code. This is technically fundamental for MALDI simulation. We report this data in Table 1 using the CHARMM formalism [1]. This data can be copied directly into the CHARMM input data.

In the MD calculations, periodic boundary conditions (toward *x-y* directions) were applied to model the MALDI evaporation at the succinic acid-vacuum interface. The crystal had a semi-infinite end toward the $-z$ direction but it was also able to evaporate toward the $+z$ spatial direction (Fig. 2). The OH bonds of succinic acid were vibrationally excited as a model for the IR laser heating. The UV excitation (i.e. an electronic transition followed by internal

Table 1a. Succinic acid topology and parameter set in CHARMM [1] format for immediate use. Additional (APPEND) data of succinic acid for CHARMM parameter set was used for the improper dihedral carbon-oxygen-carbon-oxygen motion with CHARMM commands IMPROPER / CD OB CT2 OH1 100.0 0 0.0 / END. a: Additional (APPEND) data (showing the 3-21G* level ChelpG partial charges as well) of succinic acid for CHARMM topology data set. The CHARMM format is used for convenience for those who want to use it directly in the code. Among these are that the first letter identifies the atom, the 2nd and 3rd letters or numbers identify the connection of chemical bond. In this way HOOC-CH₂-CH₂-COOH is coded as HO2-OH2-CA2(=O2)-CB2(H21)(H22)-CB1(H11)(H12)-CA1(=O1)-OH1-HO1, and “ATOM” and “BOND” keywords tell the molecular mechanics module what those mean chemically. The other keywords are CHARMM commands for the use of force field [1]

```

22      1

AUTO ANGLES DIHE

RESI SUC 0.0
GROU
ATOM HO2  H      0.44
ATOM OH2  OH1   -0.61
ATOM O2   OB    -0.55
ATOM CA2  CD     0.75
ATOM CB2  CT2   -0.21
ATOM H21  HA     0.09
ATOM H22  HA     0.09
ATOM CB1  CT2   -0.21
ATOM H11  HA     0.09
ATOM H12  HA     0.09
ATOM CA1  CD     0.75
ATOM O1   OB    -0.55
ATOM OH1  OH1   -0.61
ATOM HO1  H      0.44

BOND  HO1 OH1   OH1 CA1   O1 CA1   CA1 CB1
BOND  CB1 H11   CB1 H12   CB1 CB2
BOND  CB2 H21   CB2 H22   CB2 CA2
BOND  HO2 OH2   OH2 CA2   O2 CA2

IMPR  CA1 O1 CB1 OH1      CA2 O2 CB2 OH2
DONOR HO1 OH1
DONOR HO2 OH2
ACCE  O1 CA1
ACCE  O2 CA2
ACCE  OH1 CA1
ACCE  OH2 CA2

patch first none last none
END

```

conversion) was modeled by kinetically exciting the entire molecule (because molecular mechanics cannot account directly for electronic excitations). In the CHARMM environment, we used the Nose heating method [8, 9, 14], which not only provides correct canonical distribution functions, but also allows the application of selective heating for individual degrees of freedom (in contrast to the much simpler velocity scaling method for heating, which does neither).

In the present study, a $7 \times 7 \times 7$ unit cell size succinic acid crystal chunk was investigated (686 molecules made up of 9,604 atoms) with the guest oligonucleotide (AGCAGCT) embedded between the fourth and fifth layers of the matrix in the $+z$ direction. The entire system was prepared leaving a two unit cell size tick gap between the fourth and fifth layers where the AGCAGCT oligonucleotide (its backbone was in the *x-y* plane) was inserted. Thereafter we used a 300 K dynamical equilibration and obtained the structure depicted in Fig. 1. At this temperature the van der Waals forces are still strong enough to keep the system together, so the artificial gap closed to equilibrium distances around the analyte. (The evolution in this simulation of equilibration was followed visually on the computer screen. The equilibration was considered to be complete by seeing that the upper layers had collapsed onto

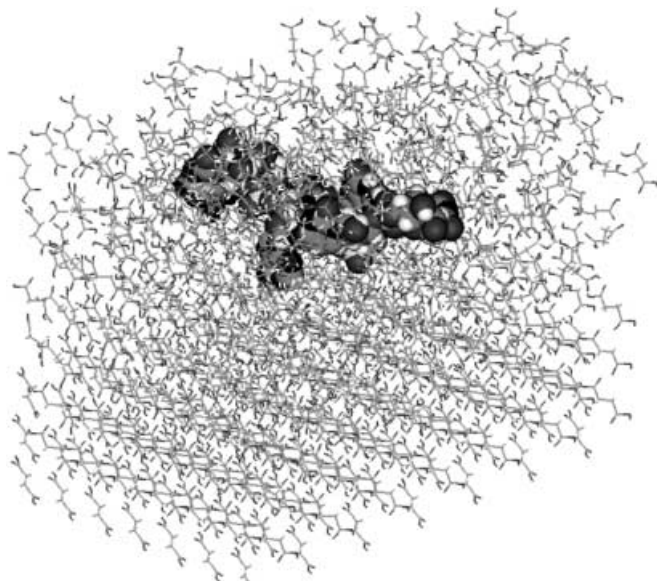


Fig. 1. A model matrix-assisted laser desorption ionization (MALDI) matrix: AGCAGCT oligonucleotide heptamer embedded in a $7 \times 7 \times 7$ unit cell size succinic acid matrix (2 succinic acids per unit cell) between the 4th and 5th layers in the $+z$ direction, and equilibrated at 300 K with molecular dynamics. Over the ordered layers, disordered layers contain the analyte. This system was evaporated thereafter by model IR and UV laser heating to 1500 K. The periodic boundary condition allowed the evaporation toward the $+z$ direction only (cf. Fig. 2). For oligonucleotide, the van der Waals radii are plotted for a better view, while for succinic acids the simple rod representation is used

the analyte and only vibration motions were visible thereafter, corresponding to 300 K.) It must be noted that while there are other possible ways to model-prepare a MALDI matrix, only speculative pictures rather than a particular experimental guideline for the exact structure of this stage are available. We believe that the structure in Fig. 1 is a reasonable starting point for MALDI.

Having this initial structure ready (Fig. 1), we applied “fast” IR heating (QREF = 100), “slow” IR heating (QREF = 2×10^9) and “slow” UV heating (QREF = 2×10^{10}). For the purpose of this article “fast” and “slow” are used to distinguish the speed of heating. The QREF is the Nose parameter (as well as CHARMM input) [1, 8], which controls the thermal coupling of the system with the outside world (heating mode). (These QREF values need to be linked to effective energy transfer, even if experimental numbers are missing: the choice of these values was done by comparing different simulations with respect to the speed of evolution of temperature of the system as a direct consequence of the QREF value. This QREF is a “slowly varying” parameter so that only its magnitude is important. We matched the time evolution of temperature to nano and pico time scale. This originated our choices for QREF.) In the slow heating (UV and IR mode), the temperature development is shown in Fig. 3a (analyzed in more detail in the next chapter), while in case of fast IR heating the temperature jumped from 300 K to 1,500 K in less than 2 ps. These two kinds of speed were supposed to model the so-called nano-laser and pico-laser excitation (heating) of the MALDI matrix. We cannot make a more detailed analysis of these numbers, because experimental data and evidence about the time-dependence of heating during MALDI processes are missing (mainly final mass spectrometric data are available on final products).

In the simulation the coordinates were saved in every 0.1 or 1 ps for later (e.g. pictorial and cluster) analysis. All the small calculations were carried out on an Indigo² workstation (Silicon Graphics, Mountain View, Calif.), and all the large calculations on a SUN

workstation at George Washington University. Molecular trajectories and configurations (e.g. Fig. 1, Fig. 2 were visualized and animated by the SCARECROW package (Centre for Scientific Computing, Espoo, Finland), which was obtained from the Internet.

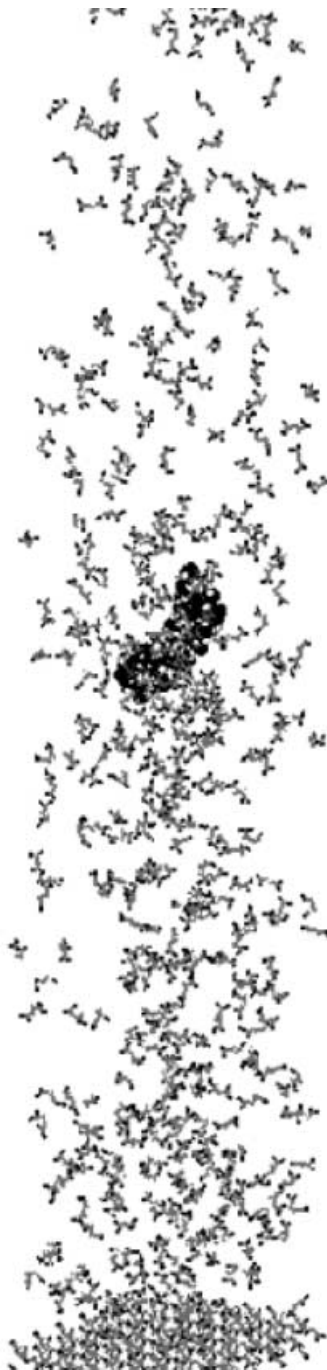


Fig. 2. Stage of evaporation of the model MALDI matrix shown in Fig. 1 at 1500 K after 100 ps. It was model heating with a slow IR laser heating mode, particularly with a QREF = 2×10^9 coupling constant (see CHARMM code [1, 8]) from 300 K, the time dependence of the temperature is depicted in Fig. 3. The selective heating method was chosen ‘à la Nose’ [8] for the OH groups of succinic acids to model the IR laser heating in this MALDI process. The cluster formation can be seen which varies with the slow or fast IR or slow UV laser heating mode described in the text. The cluster formation is analyzed in the text and in Table 2

Results and discussion

The interaction potential in CHARMM and the succinic acid parameters (Table 1) were validated by comparing the crystal structure and the enthalpy of sublimation of succinic acid to experimental data. The experimental value for the enthalpy of sublimation, 28–29 kcal/mol, was reproduced within 1 kcal/mol, probably a fortuitous result. The calculated dynamically equilibrated succinic acid structure was compared to crystallographic data determined by X-ray diffraction at 77 K and 300 K [4]. Reasonably accurate agreement was found with the largest deviation in heavy atom distances between the carboxyl carbon and the hydroxyl oxygen on the same carboxyl group (0.04 Å at 77 K and 0.05 Å at 300 K). The known zigzag structure of succinic acid crystal layers was also reproduced. Monoclinic ($a = 5.519$ Å, $b = 8.862$ Å, $c = 5.101$ Å, $\beta = 91.59^\circ$) crystal structure [4] was used throughout the CHARMM crystal build mode calculation. In addition the experimental data such as the unit cell of succinic acid crystal containing two succinic acid molecules was used (see Table 1b). These two positive test results were essential and promising, since in the MALDI process the solid structure property and the sublimation (or evaporation, see Fig. 2) play the two key roles. These two tests were a crucial precondition for our MALDI simulation.

Table 1b. Succinic acid unit cell parameters i.e. coordinates of the 28 atoms (describing two symmetry related molecules) for CHARMM crystal generation (the name SUC in the third column is optional). The second column identify the two different molecules, the 4th column identifies the atoms (first letter) and the rest describes the chemical bond connectivity like in Table 1a, necessary in molecular mechanics calculation. For accurate description we report 4 digit coordinates in columns 5–7 in “unit cell” unit [1], i.e. it must be scaled with unit cell parameters [4] if one wants to see the distances in Ångstrom for example. The last column is the temperature factor [1, 8, 9] used in the simulation

1	1	SUC	CB1	0.0808	-0.0664	-0.0277	0.16
2	1	SUC	CA1	0.2599	-0.0345	-0.2364	0.15
3	1	SUC	O1	0.2528	0.0775	-0.3760	0.18
4	1	SUC	OH1	0.4240	-0.1395	-0.2570	0.19
5	1	SUC	H11	-0.0253	-0.1635	-0.0924	0.23
6	1	SUC	H12	0.1816	-0.1035	0.1466	0.23
7	1	SUC	HO1	0.5355	-0.1189	-0.4025	0.21
8	1	SUC	CB2	-0.0808	0.0664	0.0277	0.16
9	1	SUC	CA2	-0.2599	0.0345	0.2364	0.15
10	1	SUC	O2	-0.2528	-0.0775	0.3760	0.18
11	1	SUC	OH2	-0.4240	0.1395	0.2570	0.19
12	1	SUC	H21	0.0253	0.1635	0.0924	0.23
13	1	SUC	H22	-0.1816	0.1035	-0.1466	0.23
14	1	SUC	HO2	-0.5355	0.1189	0.4025	0.21
15	2	SUC	CB1	-0.0808	0.4336	0.5277	0.16
16	2	SUC	CA1	-0.2599	0.4655	0.7364	0.15
17	2	SUC	O1	-0.2528	0.5775	0.8760	0.18
18	2	SUC	OH1	-0.4240	0.3605	0.7570	0.19
19	2	SUC	H11	0.0253	0.3365	0.5924	0.23
20	2	SUC	H12	-0.1816	0.3965	0.3534	0.23
21	2	SUC	HO1	-0.5355	0.3811	0.9025	0.21
22	2	SUC	CB2	0.0808	0.5664	0.4723	0.16
23	2	SUC	CA2	0.2599	0.5345	0.2636	0.15
24	2	SUC	O2	0.2528	0.4225	0.1240	0.18
25	2	SUC	OH2	0.4240	0.6395	0.2430	0.19
26	2	SUC	H21	-0.0253	0.6635	0.4076	0.23
27	2	SUC	H22	0.1816	0.6035	0.6466	0.23
28	2	SUC	HO2	0.5355	0.6189	0.0975	0.21

The initial MALDI matrix (Fig. 1) shows a disordered structure around the guest molecule. We think this is adequate because it is widely believed that the sample preparation method is a fast co-crystallization of the matrix and guest molecules from their saturated solution. (This is a highly non-equilibrium MALDI process.) The laser-generated volatilization of matrix crystals that follows is at the core of MALDI. This energy deposition was modeled – as described in the previous section – by kinetic excitation of the atoms of OH groups of the matrix. This simulated the IR excitation of OH groups of succinic acid molecules. The kinetic excitation of the entire succinic acid molecule simulated the UV excitation. In fact, there are other critical differences between the two modes of laser excitation, namely, the pulse width and penetration depth of the laser irradiation. These other properties affect the physics of ablation. Typical UV lasers used in MALDI have nanosecond pulse widths, hundreds of nanometers penetration depths and operate in a regime of thermal confinement. Due mainly to a longer penetration depth, typical IR lasers operate in a regime of stress confinement. Due to the limitations of CHARMM in this respect, both sets of conditions used by us are ultra-fast (i.e. instantaneous) heating – we would like to address this question in a later study. A later stage of evaporation is depicted in Fig. 2 (conditions are given in the legend). As seen in Fig. 2 the bottom layer of the sample was held rigid in the simulations (adjacent to the volume of material that has ablated). The ablation of the material causes a pressure wave into the solid and there could be a reflection of the pressure wave from the bottom of rigid layer affecting the dynamics of ablation. However, one must compromise so as not to have systems too large for such time consuming calculations.

Below we exhibit three characteristic simulations under different conditions (we have made calculations on many MD trajectories and arrangements of the analyte molecule in the matrix before our main conclusion). The statistical difference in Table 2 (discussed below in detail) shows under the column Note for the noncovalent complex between the oligonucleotide and succinic acids.

Figure 3a shows a typical temperature evolution in case of the slow IR laser heating mode. This is a highly non-equilibrium flowing (evaporating) system, and as a consequence more than one temperature can be defined. The strong fluctuation suggests that the temperatures plotted should be taken as a measure of kinetic motion. There is a continuously growing temperature difference between the internal temperature of the OH vibrations [$T(\text{OH})$] and the rest of the matrix molecule [$T(\text{matrix})$]. (The two kinds of kinetic motions – OH and the rest of the molecule – expressed in temperature were separated in the individual matrix molecules by CHARMM.) The guest temperature [$T(\text{guest})$] shows equilibrium with the matrix until phase transition occurs at ~ 70 ps. From that point on, the guest falls significantly behind the matrix in its temperature and develops a temperature difference of ~ 300 K in ~ 15 ps. This mainly comes from the increase of spatial distance between the analyte and matrix molecules during MALDI evaporation. On the

Table 2a. Theoretically calculated statistics and comparison of cluster formations in gas phase after 100 ps in the MALDI process of the sample depicted in Fig. 1 in case of different speed and mode of model laser heating. The heating started from 300 K and lasted to 1500 K. The number of atoms in the system is $N(\text{atom})=9832$, including the atoms of numerous ($7 \times 7 \times 7$ unit cell) succinic acids and one guest (AGCAGCT) molecule. Notations: i = the size of

i (cluster size)	$N(i)$	$N(i)/N(\text{cluster})$ (piecewise ratio)	$i \cdot N(i)/N(\text{atom})$ (integrated volume ratio)	Note
14	339	0.833	0.483	SUC monomer
28	44	0.108	0.125	SUC dimers
42	10	0.025	0.043	SUC trimers
56	8	0.020	0.046	SUC tetramers
70	4	0.010	0.028	SUC pentamers
452	1	0.002	0.046	oligo(228 atoms) + 16 SUC
2254	1	0.002	0.229	161 SUC remained on surface

the cluster, $N(i)$ = the number of clusters with this size (i), $N(\text{cluster})$ = number of individual clusters (irrespective of size), and SUC = succinic acid. The succinic acid contains 14 atoms, so multiples of number 14 in the table immediately refer to the succinic acid clusters or multiples. a: "Slow" ($Q_{\text{REF}} = 2 \times 10^9$) IR heating of OH in the carboxyl groups of succinic acid. $N(\text{cluster}) = 407$

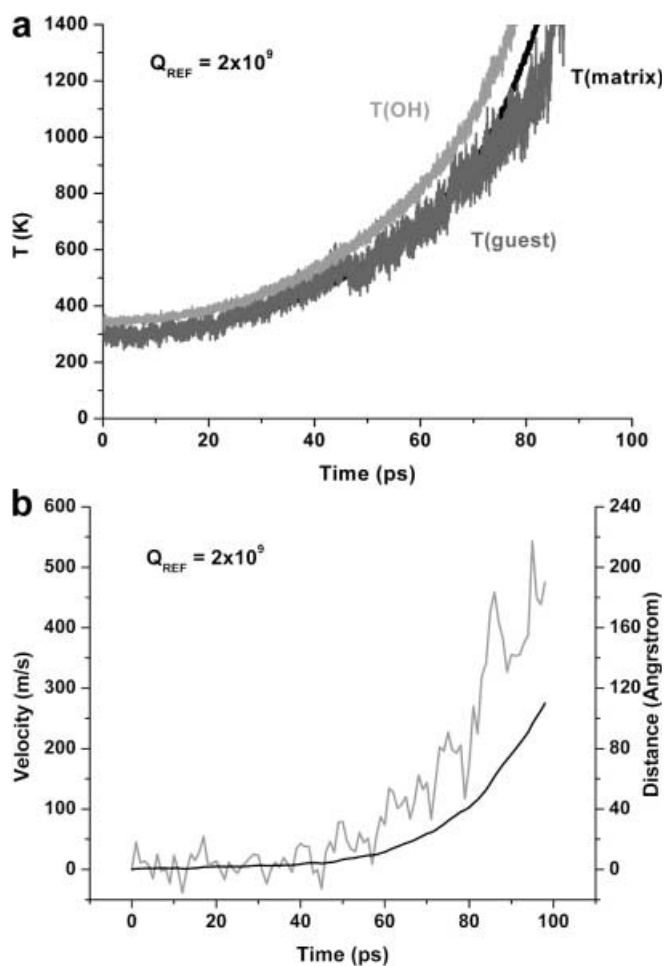


Fig. 3. **a** The time dependence of the temperature in MALDI process during a selective slow IR laser excitation (thermal coupling) of OH groups (cf. $T(\text{OH})$) of succinic acids shown in Fig. 2. The $T(\text{matrix})$ and $T(\text{guest})$ are the temperatures of the remaining part of the succinic acid molecule as well as the analyte. These latter two were heated via mechanical coupling to the OH groups of succinic acids in this non-equilibrium flowing system. The evaporation started around 50 ps. (The temperatures were calculated by CHARMM subroutine from kinetic properties of the system). **b** The distance of the center of mass of oligonucleotide (guest) from its original position at $t = 0$ as well as its time derivative, the lift off velocity (upper curve) – notice the different scales marked on both sides

other hand, the slow UV heating mode (not plotted) proceeds through uniform excitation of the internal degrees of freedom of succinic acid molecules. The matrix and guest temperatures are closely correlated until phase transition occurs similarly at ~ 70 ps. From this point on, rapid divergence is observed between the two temperatures [$T(\text{guest})$ and $T(\text{matrix})$, where in this UV heating mode the latter refers to the entire succinic acid molecule] leading to a difference of ~ 700 K in ~ 15 ps. An interesting part of the development of the $T(\text{matrix})$ curve shown in Fig. 3a for the slow IR heating mode is the visible jump which can be observed around 50 ps, the time when guest starts to lift off. This kind of behavior was observed in other systems as well as in the slow UV heating mode. Unfortunately, there is no experimental data on the transient internal temperature of matrix molecules immediately after the laser pulse.

Our calculation has also yielded lift off velocities and traveling distances for the analyte, plotted in Fig. 3b for the slow IR heating mode. No particular measured values are available for comparing the lift off velocities shown in Fig. 3b, but at least we know that the values shown in this figure are of the magnitude that experiments generally yield. Based on the density and temperature history of the system, the actual collision frequency between the matrix and guest species can be calculated. Although this is a non-equilibrium system, the known general equation for collision frequency between succinic acid and guest can yield the correct magnitude. Particular values have been reported elsewhere; see [15]. The collision frequency during the first ~ 50 ps of heating is similar to condensed phase values. Following this period a phase transition (evaporation) occurs and the collision frequency drops precipitously. In the fast IR heating mode, the $T(\text{OH})$ temperature reached 1,500 K in less than 2 ps, and maintained a constant value with time, and via energy transfer from these OH vibrations, the $T(\text{matrix})$ jumped up to $\sim 1,130$ K in less than 2 ps. In addition the $T(\text{guest})$ jumped up to $\sim 1,100$ K in about 5 ps and maintained a constant value with a similar fluctuation as in Fig. 3a. As a consequence of the jump in temperature, the guest, along with many succinic acid molecules were leaving the surface instantly.

As indicated in the title, we compared the cluster formation among succinic acid molecules as well as succinic acid molecules and guest molecules in relation to different model laser heating modes. This is summarized in Table 2. For this MALDI modeling, we defined the cluster as follows: two atoms belong to the same cluster if the distance between them is less than 3.0 Å. Of course, if the distance is larger they may or may not belong to the same cluster. In this way, chains (possibly with side chains) of atoms form larger clusters via these adjacent atoms, which satisfy this condition pairwise. In particular, all individual succinic acid molecules and guest molecules form clusters, because the chemical bonds between their atoms are shorter than this 3 Å distance in the cluster definition. However, if two molecules get close to each other in a way that any one atom of the first is close to an atom of the second molecule, i.e. they are within this 3 Å distance, these two molecules are considered as belonging to the same bigger cluster. This is more interesting to us, because in this cluster there are not only chemical bonds, but van der Waals bonds (non covalent bonds) as well. This 3.0 Å value is arbitrary and may be questionable as a rigorous definition in the early phase of evaporation when all the molecules are close together. However, as the clusters have already been formed and separated well apart from each other (e.g. 100 ps after the evaporation), seeking a more accurate value than 3.0 Å is irrelevant (cf. Fig. 2, 3 and Table 2). For example a 2.9 or 3.1 Å value would define the same spectrum of cluster size distribution in Table 2. (Too small a value, e.g. 0.1 Å, would result in only one atom belonging to a cluster, while too large a distance would make the entire system one big cluster. The origin of this 3 Å value is that it is an upper limit of any chemical bond length or a lower limit of a van der Waals distance.)

Table 2 shows the cluster formation statistics in case of slow IR (Table 2a), fast IR (Table 2b) and slow UV laser heating mode of the model MALDI system 100 ps

after the laser pulse started. The center of mass of the guest molecule from the surface was about 110, 450, and 250 Å respectively in these cases and can be considered as a gas phase particle. (The larger 450 Å value comes from the obvious fact that in the case of fast IR heating, the guest lifted off from the surface instantly.) Table 2 reveals that the three distributions of clusters are quite distinguishable in these different heating modes. The number of clusters, $N(\text{cluster})$, are 407, 380 and 478 respectively, while the number of individual succinic acid molecules are 339, 334 and 430 respectively. The low $N(\text{cluster})$ value in the second (fast IR heating) case is because many succinic acids remained on the surface (226, cf. Table 2b) – it is interesting, because in this case the temperature jump (or laser energy transfer) to 1,500 K was almost instantaneous. On the other hand, the slow IR and slow UV laser heating mode provided about the same temperature slope (cf. Fig. 3a) in contrast to the fast IR heating temperature jump. But still, the IR mode (slow or fast) produced less individual succinic acid gas phase molecules (339 or 334) than the UV laser mode (430). Careful explanation of these results is needed. We think that the explanation may be as follows: the UV heating, targeting the entire succinic acid molecule, shakes the matrix molecules off from the MALDI ensemble more effectively than the IR heating which targets only a particular group (here, OH) of the molecule. The largest gas phase matrix clusters are succinic acid pentamers, 19-mers and 5-mers respectively, while the numbers of succinic acid molecules adhering to the guest molecule are 16, 11 and 2 respectively. The 19-mer peak is again interesting, since it seems to us that the fast IR laser pulse can cut off large chunks from the solid phase MALDI matrix. It is also characteristic that the UV laser heating causes much less (about 5–8 times) succinic acids to adhere to the guest molecule than the IR laser heating mode, which quite obviously comes from the different nature of energy coupling between molecules or subgroups.

Table 2b. “Fast” (QREF = 100) IR heating of OH in the carboxil groups of succinic acid. $N(\text{cluster}) = 380$

$i(\text{cluster size})$	$N(i)$	$N(i)/N(\text{cluster})$ (piecewise ratio)	$i*N(i)/N(\text{atom})$ (integrated volume ratio)	Note
14	334	0.879	0.476	SUC monomer
28	36	0.095	0.103	SUC dimer
42	4	0.011	0.017	SUC trimer
56	3	0.008	0.017	SUC tetramer
266	1	0.003	0.027	SUC 19-mer
382	1	0.003	0.039	oligo (228 atoms) + 11 SUC
3164	1	0.003	0.322	226 SUC remained on the surface

Table 2c. “Slow”(QREF = 2×10^{10}) UV heating of succinic acid. $N(\text{cluster}) = 478$

$i(\text{cluster size})$	$N(i)$	$N(i)/N(\text{cluster})$ (piecewise ratio)	$i*N(i)/N(\text{atom})$ (integrated volume ratio)	Note
14	430	0.900	0.612	SUC monomer
28	38	0.079	0.108	SUC dimers
42	6	0.013	0.026	SUC trimers
56	1	0.002	0.006	SUC tetramers
70	1	0.002	0.007	SUC pentamers
256	1	0.002	0.026	oligo(228 atoms) + 2 SUC
2114	1	0.002	0.215	151 SUC remained on surface

This cluster analysis can serve as theoretical spectra to help to explain the experimental mass spectra obtained in MALDI experiments. Further investigations are needed to explore more details about the energy transfer between molecules in MALDI which may enable us to better understand the MALDI process, as well as to predict its mass spectra theoretically.

Acknowledgements. The authors are thankful for the financial support from the National Science Foundation (USA) and OTKA (Orszagos Tudomanyos Kutatasi Alap, Hungary).

References

1. Brooks BR, Bruccoleri RE, Olafson BD, States DJ, Swaminathan S, Karplus M (1983) *J Comput Chem* 4: 187
2. Bencsura A, Vertes A (1995) *Chem Phys Lett* 247: 142
3. Zhigilei LV, Kodali PBS, Garrison BJ (1998) *J Phys Chem B* 102: 2845
4. Leviel J, Auvert G, Savariault J (1981) *Acta Crystallogr B* 37: 2185
5. Tang X, Callahan JH, Zhou P, Vertes A (1995) *Anal Chem* 67: 4542
6. Schmidt MW, Baldrige KK, Boatz JA, Elbert ST, Gordon MS, Jensen JJ, Koseki S, Matsunaga N, Nguyen KA, Su S, Windus TL, Dupuis M, Montgomery JA (1993) *J Comput Chem* 14: 1347
7. Breneman CM, Wiberg KB (1990) *J Comput Chem* 11: 361
8. Nose S (1984) *J Chem Phys* 81: 511
9. Hoover WG (1985) *Phys Rev A* 31: 1695
10. Kristyan S, Ruzsinszky A, Csonka GI (2001) *J Phys Chem A* 105: 1926
11. Kristyan S, Csonka GI (2001) *J Comput Chem* 22: 241
12. Kristyan S, Csonka GI (1999) *Chem Phys Lett* 307: 469
13. Kristyan S *Chem Phys* (1997) 224: 33
14. Branka A, Parrinello M (1986) *Mol Phys* 58: 989
15. Kristyan S, Vertes A (2000) American Society for Mass Spectrometry, 2000 Jun 10–15 Conference